Water Biology and Security xxx (xxxx) xxx

Contents lists available at ScienceDirect

Water Biology and Security

journal homepage: www.keaipublishing.com/en/journals/water-biology-and-security

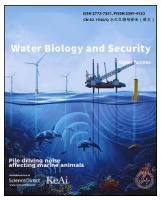

Research Article

High-resolution holographic reconstruction combined with fluorescence microscopy to identify unwanted *Chlorella* sp. cells in *Haematococcus pluvialis* cultures

María Salinas-García[a,b], Barbara Bicsák[c], Gabriel Acién[a,b], Tomás Lafarga[a,b,*]

[a] Department of Chemical Engineering, University of Almeria, 04120, Almeria, Spain
[b] CIESOL Solar Energy Research Centre, 04120, Almeria, Spain
[c] HUN-REN SZTAKI, 13-17 Kende Street, 1111, Budapest, Hungary

ARTICLE INFO

Keywords:
Artificial intelligence
Fluorescence microscopy
High resolution holographic reconstruction
Culture monitoring
Novel sensors
Image analysis

ABSTRACT

This study evaluated the performance of HOLODETECT HiRes + FLUOR3, a laboratory instrument designed for detecting and counting small particles or cells in fluids using fluorescence. The test species were *Haematococcus pluvialis* and *Chlorella sorokiniana* because of their industrial importance in the functional food markets, and because they have been identified growing in co-culture, especially when the goal is to produce *H. pluvialis*. Initial trials focused on optimising the operating conditions to ensure accurate and reproducible measurements. The equipment demonstrated a low coefficient of variation (<5 %) for all the different determinations. Due to cell overlap, sample dilution was necessary in dense cultures prior to analysis. A second set of trials aimed to develop models (i) to identify the cell concentration in monocultures and co-cultures, and (ii) to determine the relative abundance of the two test species in mixed cultures. The models that were developed were able to provide cell count results comparable to those obtained using a Neubauer counting chamber. However, the model development step proved to be important, as different modelling approaches led to different results with some models overestimating and others underestimating the total cell count. Similarly, the system accurately quantifies the relative abundance of *C. sorokiniana* and *H. pluvialis* cells in cultures with different cell concentration ratios.

1. Introduction

Microalgal production has attracted significant interest across various industries due to the photosynthetic nature of microalgal biomass, and its potential applications. Today, several microalgae-based metabolite production processes have achieved commercial success; for example, phycocyanin from *Arthrospira platensis* Gomont, 1892 and β-carotene from *Dunaliella salina* (Dunal) Teodoresco, 1905 are commercially available.

Microalgae are mainly produced autotrophically using open bioreactors, with raceway ponds being the most used design. Raceways have been used for over 50 years to produce both *A. platensis* and *D. salina,* taking advantage of the fact that the growth conditions for these microalgae are unsuitable for most competing species. The former is produced using high concentrations of sodium bicarbonate, with a pH generally around 10 (Villaró-Cos et al., 2024), while the latter is produced using sea salt, as it can grow well in media with a conductivity higher than 150 mS cm^{-1} (Colusse et al., 2020). Producing other strains in raceway reactors is challenging because of the appearance of unwanted fast-growing competing species that can dominate the culture. For example, a metagenomic analysis showed that an unwanted microalga was the most abundant in an open bioreactor that had been inoculated with *Scenedesmus almeriensis* approximately one month earlier (Villaró et al., 2022). Even reactors inoculated with extremophile species and strains can be contaminated with unwanted microalgae or with algal predators such as protozoa, rotifers, and ostracods. For example, *Alkalimonas* sp. and *Lentimonas* sp., as well as an unclassified metazoan, have been found in cultures of *A. platensis* (Villaró et al., 2023).

The appearance of contaminating species in microalgal cultures has

* Corresponding author. Department of Chemical Engineering, University of Almeria, 04120, Almeria, Spain.
E-mail address: lpt365@ual.es (T. Lafarga).

Peer review under the responsibility of Editorial Office of Water Biology and Security.

https://doi.org/10.1016/j.watbs.2025.100546
Received 25 May 2025; Received in revised form 29 July 2025; Accepted 31 December 2025
Available online xxxx

Please cite this article as: Salinas-García, M. et al., High-resolution holographic reconstruction combined with fluorescence microscopy to identify unwanted *Chlorella* sp. cells in *Haematococcus pluvialis* cultures, Water Biology and Security, https://doi.org/10.1016/j.watbs.2025.100546

been overlooked in the scientific literature. Despite the presence of algal predators in large cultures being recognised since the 1960s, most of the works published to date have been carried out using laboratory-scale reactors. At the laboratory-scale, the culture conditions can be easily controlled (e.g., by autoclaving the culture medium), and the appearance of competing strains and/or algal predators is not generally a problem. However, over the last two decades, several microalgal-based production processes have been upscaled and the presence of predators and competing microorganisms has become an important challenge for microalgae producers.

Chlorella vulgaris Beijerinck, 1890 and *Chlorella sorokiniana* Shihira and Krauss, 1965 are microalgae of industrial importance since they can be used as human food. They are approved as food by the FDA in the US and by EFSA in the EU and there are several products containing *Chlorella* sp. already available on the market. Despite being fast-growing microorganisms, they are not extremophiles so producing them in open systems is challenging. Moreover, because of their high growth rate, *Chlorella* sp. can overtake cultures or other species. For example, *Chlorella* sp. cells in *Haematococcus pluvialis* Flotow, 1844 cultures can prove problematic when the goal is to produce astaxanthin. Other species, such as *Chlamydomonas reinhardtii* Dangeard, 1888, also act as biotic contaminants of *H. pluvialis* cultures (Yu et al., 2022). Various methods have been investigated to stop or limit the growth of unwanted microorganisms. For example, pyraclostrobin-based fungicides and the anionic surfactant sodium dodecylbenzene sulfonate have been investigated to control fungal contaminants in cultures of *Scenedesmus dimorphus* (Turpin) Kützing, 1834 and *Graesiella* sp. Kalina and Puncochárová, 1987, respectively (Ding et al., 2020). Adjusting the pH has also been assessed as a method to control the growth of unwanted microorganisms in cultures of *H. pluvialis* (Hwang et al., 2019) and a combination of botanical pesticides was investigated for exterminating rotifers in cultures of *A. platensis* (Huang et al., 2014).

To implement effective contingency measures and combat unwanted microorganisms, it is crucial to first identify the contaminant. The sooner the contaminant is detected, the greater the chances of controlling its growth. Therefore, it is important to develop and implement online monitoring tools that can detect the appearance of unwanted microorganisms, including microalgae, in industrial cultures. Various methods are now being studied, including AI-based models, to detect contamination based on spectrophotometry (González-Hernández et al., 2025). In this study, the authors evaluated the performance of HOLODETECT HiRes + FLUOR3 (Holodetect Instruments Ltd., Budapest, Hungary), a laboratory instrument for detecting and counting small particles or cells in fluids using fluorescence. The test strains were *H. pluvialis* and *C. sorokiniana* because of their industrial importance and because they have both been identified growing in co-culture when the goal was to produce one or the other.

2. Materials and methods

2.1. Microalgal cultures

The test species belonged to the genera *Haematococcus* and *Chlorella*. For *Haematococcus*, the species used was *H. pluvialis*, sourced from several culture collections, including 1360B BEA, BMCC 673, Algaria (Italy), SAG 192.80, and CCCryo 096–99. The species of *Chlorella* that was used was *C. sorokiniana* that had been adapted to seawater and collected from cultures grown and cultivated under a range of conditions in a variety of photobioreactor systems, including tubular reactors. The two species were subsequently grown in 1 L controlled bubble columns (pH 8.0; 25 °C) at a constant aeration of 0.2 v/v/min and photon irradiance of 350 μmol photons·(PAR)·m^{-2}·s^{-1} measured using an US-SQS spherical quantum sensor (Walz, Effeltrich, Germany). Light was provided using 13.3 W LEXMAN LED tubes (Leroy Merlin, Madrid, Spain). The culture medium was prepared using 0.90 g L^{-1} $NaNO_3$, 0.14 g L^{-1} KH_2PO_4, 0.18 g L^{-1} $MgSO_4$ and 20 mg L^{-1} Karentol® Mix Super (Kenogard, Barcelona, Spain), a commercial micronutrient mixture (Morillas-España et al., 2020). The cultures were diluted when needed using fresh culture medium. The biomass concentration was calculated gravimetrically. Briefly, 30 mL of culture was filtered through pre-dried 0.45 μm filters and washed with 60 mL of distilled water to remove the salts then dried in an oven at 80 °C for 24 h following UNE-EN 17605 (UNE, 2022). In addition, the cell concentration was calculated using a Neubauer counting chamber (NCC) and a Leica DM 750 microscope coupled with a Flexacam i5 camera using Enersight software (Leica Microsistemas, Barcelona, Spain).

2.2. High-resolution holographic reconstruction combined with fluorescence microscopy

The first set of trials evaluated the performance of the Holodetect HiRes + Fluor3 (HF3) device in detecting and classifying microalgal cells, and to determine whether sample dilution was required prior to analysis.

The system integrates digital holographic microscopy (DHM), providing a holographic resolution of 600 nm, with multi-wavelength fluorescence microscopy (excitation at 405 nm, 450 nm and 532 nm). In recent years, this combined approach has been explored for microalgae characterisation, and enhanced methods have been developed which capture both morphological and biochemical features simultaneously (Yourassowsky et al., 2024). Liquid samples were analysed within a flow-through cuvette at a depth of 200 μm and at a flow rate of between 3.6 μL min^{-1} and 18 μL min^{-1} depending on the culture's cell concentration. The HF3 technology captures the entire 200 μm depth of a sample in a single holographic image, eliminating the need for optical refocussing and allowing the reconstruction of all objects within the detectable size range of 3 μm–75 μm. The flow cell used to pass the sample through the system is a rectangular glass slide with a central tube. The slide is arranged in a vertical position with a silicone tube affixed at both ends and connected to a peristaltic pump. The sample is passed through the flow cell, where two cameras record the images, with the holographic image of the sample having to be registered with the fluorescence image. Instrument-level parameters, such as camera magnification, rotation, and laser light distribution, must be optimised during the equipment set-up. Slight dynamic offsets can be introduced by operational factors. This is a common challenge in systems that integrate fluorescence and imaging. For instance, the FlowCAM device incorporates a laser in fluorescence triggered mode, which requires calibration of the gain and threshold settings, among others (Chen et al., 2023; Jaffari et al., 2024).

To ensure the accuracy of the HF3 equipment, an automatic calibration routine is performed prior to each use. For this calibration, a sample of the fresh culture is introduced, allowing the system to automatically calculate and compensate any offset. This ensures the correct overlap between the reconstructed holographic object and its corresponding fluorescence signal.

To determine the optimum cell concentration to allow accurate counting, samples of *C. sorokiniana* and *H. pluvialis* cultures were analysed using both HF3 and NCC to compare reliability and reproducibility. Each culture was serially diluted until the system could accurately distinguish individual cells, even in cases of partial cell overlap. At each dilution step, cell concentration was measured using both methods, and dry weight measurements was also measured. This process was repeated until the cell concentration became too low for a reliable counting threshold using either method.

Furthermore, the minimum number of objects required to achieve reproducible results was determined by modifying the system's “number of objects to be measured”, ranging from 375 to 6000 objects per measurement. Subsequent counts were performed using NCC for comparative analysis.

2.3. Model generation

HF3 employs deep neural networks (DNNs) implemented in PyTorch (v2.2.0 with CUDA 11.8 support) for automated classification (Paszke et al., 2019) and trained using a staged few-shot learning approach (Wang et al., 2023). Three different models were developed in this study. Two of them were trained using monocultures of *C. sorokiniana* and *H. pluvialis* separately. The use of pure cultures to generate the model ensured accurate cell labelling with this approach, as no other microalgae were present. To create the database, only the target species was manually annotated in each case. This resulted in two species-specific models, one for *C. sorokiniana* and the other for *H. pluvialis*, in which all non-target particles were labelled as "others". A third model was generated by labelling both species independently within the same training dataset, allowing direct discrimination between them.

For each model, initial training was performed on small, annotated datasets (approximately 10 objects per class). A preliminary model was trained and used to pre-classify additional detected objects, employing semi-supervised iterations where preliminary model predictions were manually corrected and reintroduced into the training set. This allowed the training database to be expanded and refined. The built-in annotation tool facilitated labelling based on holographic morphology and fluorescence signals. This semi-supervised iterative approach helped to improve classification accuracy while minimising manual labelling effort.

The final annotated datasets were randomly divided into training (70 %), validation (15 %), and test (15 %) sets, with the only requirement being that each set contain an equal number of elements of each class to avoid bias in the training. The validation set was held out during training to prevent overfitting, with model training automatically stopping when validation accuracy plateaued. The DNN architecture incorporated both holographic and fluorescence data, with inputs standardised to the same size (128 pixels), since the model has a uniform and invariable input size.

2.4. Model validation

Model validation was conducted using pure monocultures of *C. sorokiniana* and *H. pluvialis* (distinct from the samples used for model training), with cell concentrations accurately determined using the NCC. The use of pure cultures ensured that no unwanted species interfered with the model specificity assessment. From these quantified cultures, six standardised cellular mixtures were prepared: 10 % *C. sorokiniana* (90 % *H. pluvialis*), 25 % *C. sorokiniana* (75 % *H. pluvialis*), 50 % *C. sorokiniana* (50 % *H. pluvialis*), 75 % *C. sorokiniana* (25 % *H. pluvialis*), 90 % *C. sorokiniana* (10 % *H. pluvialis*), and 100 % of each species. These mixtures were designed to represent a range of contamination levels, from highly contaminated to pure cultures, simulating the contamination scenarios that may be present in commercial microalgal culture systems.

Each mixture was analysed using all three classification models to evaluate their performance under the full range of species abundance ratios. The number of cells analysed per sample corresponded to the previously established optimal object count to ensure accuracy and reproducibility across replicates. The aim was to evaluate the ability of each model to correctly identify, quantify and classify both species over a range of relative abundances. The model outputs were compared with the expected ratios derived from manual cell counts. This validation procedure enabled a comprehensive assessment of each model's generalisability and its ability to detect and quantify target species in mixed cultures.

2.5. Statistical analysis

Data were analysed using a one-way analysis of variance and a Fisher's LSD post hoc test ($p < 0.05$) using Statgraphics Centurion v19 (Statgraphics Technologies Inc., VA, USA) software.

3. Results and discussion

As previously explained, the presence of contaminating microorganisms such as microalgae in *Chlorella* sp. and *Haematococcus* sp. cultures is a common issue that poses a challenge at the commercial scale. These microorganisms may present a health risk or could compromise the quality of the product produced. For instance, in the case of *Haematococcus* sp., growth of competing species can lead to reduced astaxanthin production. When this occurs, it is essential to implement control measures, such as filtration, to eliminate or limit the growth of the undesired contaminating species. The earlier these measures are implemented, the better. Therefore, the adoption of online monitoring tools capable of identifying different species or microorganisms is crucial. In this study, *C. sorokiniana* and *H. pluvialis* were used as model organisms, and the HF3, was validated for the first time.

3.1. Equipment calibration

HF3 utilises digital holographic microscopy and artificial intelligence to detect, classify and count cells and objects ranging in size from 3 μm to 75 μm. The primary objectives of the trials in this initial study were (i) to assess the device's ability to detect and classify cultures with different cell concentrations, and (ii) to determine the minimum number of reads required to obtain reproducible results.

The first objective is particularly important given that, in concentrated cultures, some cells may overlap, requiring sample dilution before readings to ensure accurate analysis. This was observed in previous studies where overlapping cells or cell aggregates limited the accuracy of techniques such as flow cytometry, plate counting, or electron microscopy (Di Caprio, 2020). Cultures containing different relative cell concentrations of *C. sorokiniana* and *H. pluvialis* were analysed using both HF3 and NCC. The results are shown in Fig. 1. For the *C. sorokiniana* cultures, a positive correlation was observed between the cell concentration assessed using HF3 and NCC ($p < 0.05$; 0.9773). The biomass concentration ranged between 0.00 g L^{-1} and 0.06 g L^{-1}; higher cell concentrations led to cell overlap and to larger differences between the two counting methods. In turn, *H. pluvialis* could be counted at higher cell concentrations using HF3, but with minor differences observed between the results obtained using HF3 and NCC at a biomass concentration of approximately 1 g L^{-1}. In this case, a positive correlation was observed between the cell concentration calculated using HF3 and NCC in cultures with biomass concentrations ranging from 0.0 g L^{-1} to 1.1 g L^{-1} ($p < 0.05$; 0.9889). Despite the biomass concentration (g·L^{-1}) being higher, the cell concentration (cells·L^{-1}) in both cultures was of the same order of magnitude. The reason for this is the difference in cell biovolume because the diameter of *C. sorokiniana* is between 2 μm and 5 μm, while the diameter of *H. pluvialis* is between 10 μm and 60 μm (Baroni et al., 2019). The need to dilute denser cultures is also required in other cell counting methods. Similarly, in a previous study, the authors reported greater noise in the data computed from images of a flow-through microscope at the end of the growth phase (50–60 cells per image) than at the beginning (less than 10 cells per image). In that study, the authors filtered the data using a 12-h asymmetric median to obtain a smoother output (Havlik et al., 2013). Overall, cell concentration influenced the accuracy of the results ($p < 0.05$). For concentrated cultures, a dilution step might be necessary to correctly estimate biomass concentration and identify contaminants. These results are in line with those observed in systems such as FlowCam. When operating a FlowCam at higher cell concentrations, overlapping has been observed, which can lead to errors of up to 14.8 % when compared to traditional microscopy methods (Álvarez et al., 2011). The dilution step might not be necessary for larger microalgae such as *H. pluvialis*, where the system was able to accurately calculate the cell concentration at a biomass concentration higher than 1 g L^{-1}.

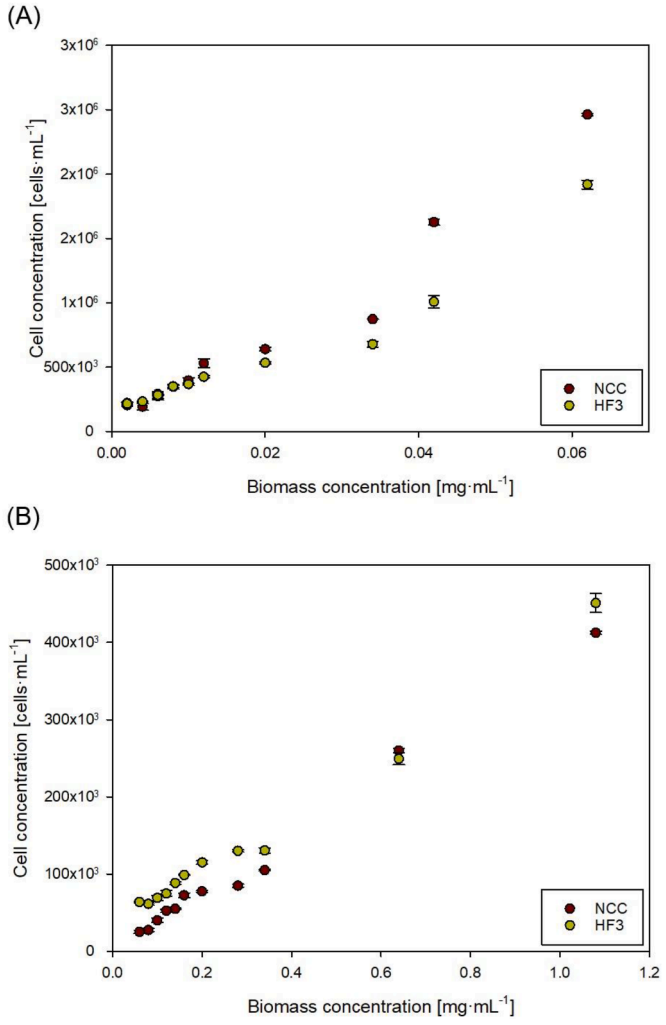

Fig. 1. Effect of the biomass concentration on the performance of HF3 when analysing cultures of (**A**) *C. sorokiniana* and (**B**) *H. pluvialis*. HF3 and NCC refer to HOLODETECT HiRes + FLUOR3 and Neubauer counting chamber, respectively. The results are the average of five independent determinations per species ± SD.

The second objective of these initial trials was to determine the minimum number of read objects needed to achieve accurate and reproducible results. To accomplish this, multiple measurements of the same sample were taken under consistent conditions, with a different number of objects read for each sample (ranging from 375 to 6000). The results are shown in Fig. 2. Overall, no differences were observed in the CV values obtained for either species, being below 5 % in all the analysed samples. However, the number of read objects had an impact on the CV, which decreased from 2.3 to 0.3 in *C. sorokiniana* cultures when 375 and 6000 objects were read, respectively ($p < 0.05$). Similarly, the CV decreased from 3.9 to 1.9 in *H. pluvialis* cultures when 375 and 6000 objects were read, respectively ($p < 0.05$). For both species, no differences were observed between the CV obtained when measuring 1500 objects or more, suggesting that measuring 1500 objects per sample is enough to achieve reproducible results. Even if a lower number of objects is counted, the maximum CV value obtained was below 5 %. The number of objects analysed per sample is important because the higher this value, the lower the statistical error reduction factor, which is relevant in biological processes where higher cell concentrations result in reduced effects. The accuracy of the results was also calculated by comparing the number of objects read using HF3 and NCC. Overall, the larger the number of objects analysed, the lower the discrepancy between the results obtained using HF3 and NCC. The same occurred when using both *C. sorokiniana* and *H. pluvialis*. When just 375 objects were analysed per sample, the difference between the data obtained using HF3 was between 15 % and 20 % but only 10 % when 6000 objects per sample were analysed ($p < 0.05$).

These first trials demonstrated that the higher the number of objects detected, the greater the reproducibility of the results and the lower the difference between HF3 and NCC. However, no statistically significant improvements were observed when 6000 objects were measured compared to 1500. Regardless of the number of objects analysed, the CV was below 5 % in all the samples, indicating very high precision and reproducibility. Nonetheless, one limitation identified was the need to dilute the *C. sorokiniana* cultures since cell concentrations higher than 2×10^6 cells·mL^{-1} led to lower accuracy; this is because cell overlap made it challenging for the software to resolve individual cells. The same problem was found by Sarrafzadeh et al. (2015) who compared different methods for measuring biomass concentrations in microalgal cultures. In the case of *C. sorokiniana,* a cell concentration of 2×10^6 to 3×10^6 cells·mL^{-1} represents a biomass concentration of approximately 0.04–0.06 g L^{-1}, which can be easily reached in laboratory-scale photobioreactors as well as in large-scale systems. Therefore, to use HF3 as an online monitoring system in large-scale systems, an automatic dilution step might be needed depending on the species being produced. This study demonstrated that the HF3 system has the capability to distinguish between different microalgal species by training with species specific image libraries. The system can be adapted to identify between

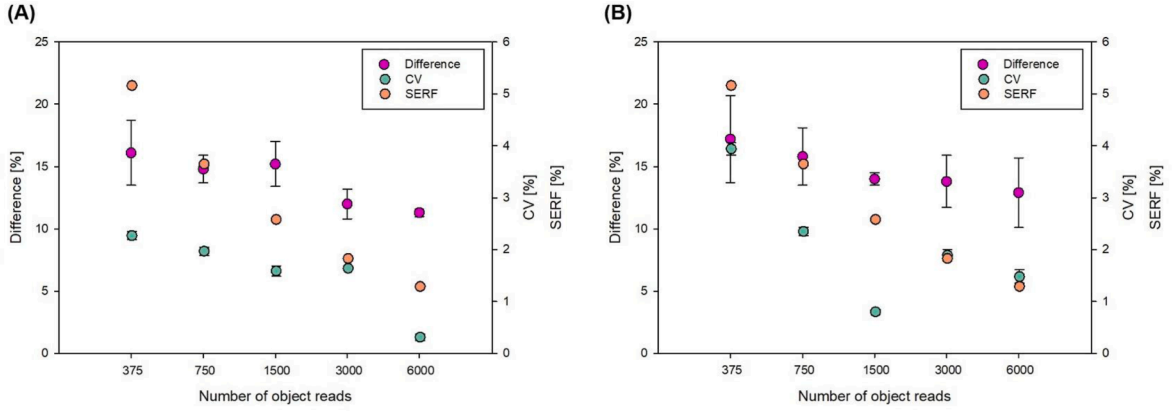

Fig. 2. Effect of the number of objects identified on the difference between the HF3 results and a Neubauer counting chamber, the coefficient of variation (CV) and the statistical error reduction factor (SERF) in cultures of (**A**) *C. sorokiniana* and (**B**) *H. pluvialis*. Values represent the mean value of five independent determinations ± SD.

species under different conditions, provided that the morphological characteristics are sufficiently distinctive and adequate training data are available.

3.2. Model development

Two different methodologies were followed: (i) developing monoculture models for each species and (ii) developing a co-culture model where both species were considered. The models that were developed using monocultures of *C. sorokiniana* and *H. pluvialis* cells were called M1 and M2 respectively while the co-culture model where both strains were considered independently within the same culture was called M3. When developing M1 and M2, the objects counted as "others" were mainly *C. sorokiniana* cells in the *H. pluvialis* M2 model, and mainly *H. pluvialis* cells in the *C. sorokiniana* M1 model. The M1 and M2 models were developed on the hypothesis that a model focused on a single species would enhance the sensitivity to detect the target organism while minimising potential particle noise interference. Conversely, M3 was developed based on the hypothesis that integrating both species into one model would yield greater robustness in complex environments with mixed species.

The imaging system that was used generates two complementary types of data for each field of view: a holographic reconstruction and the fluorescence signals emitted by the sample. Model M1 tended to overestimate the number of *C. sorokiniana* cells because it misclassified noncellular particles and environmental debris as target cells. This limitation was largely attributed to the model's reliance on chlorophyll autofluorescence signals, particularly the red fluorescence ('FLUOR_INTENSITY_RED') emitted, which is known to be susceptible to interference by external fluorescence sources and particulate matter. As previously reported, the red fluorescence channel cannot clearly distinguish between chlorophyll signals and other fluorescent emissions, making a precise classification difficult (Takahashi, 2019). The model also relies on morphological parameters, including area and perimeter ('MASK_AREA' and 'MASK_PERIMETER'), focuses on the photosynthetic pigment profile and cell dimensions characteristic of *C. sorokiniana*.

In contrast, the M2 model, developed using pure *H. pluvialis* cultures, shows better specificity in detecting *H. pluvialis* cells, due to the significant difference in cell size compared to *C. sorokiniana*. The model was trained with samples containing all the physiological phases of *H. pluvialis*, including motile and vegetative green cells, and non-motile red cells. Recognising different sizes of *H. pluvialis* cells in all their phases, the model incorporated a size-based filter with non-motile cells typically being from 10 μm to 50 μm and motile cells typically 5 μm–30 μm (Zhang et al., 2017) in diameter. The filter used MASK_MINENCCIRCDIAMETER (36.13 ± 30.92 μm), which allowed the model to effectively exclude small particles and contaminants, such as *C. sorokiniana* (which has a cell size less than 5 μm), from being misclassified as *H. pluvialis*. Despite better discrimination, there were still challenges in distinguishing between aggregates of small cells such as *C. sorokiniana* and individual *H. pluvialis* cells. This showed that while size filtering improved specificity, it was not sufficient to distinguish all the cells in a mixed culture.

The third model, M3, was developed to address the limitations of the M1 and M2 models. This was achieved by considering both *C. sorokiniana* and *H. pluvialis* as independent classes during model training. This integrated model took advantage of multiple fluorescence channels ('FLUOR_INTENSITY_RED' and 'FLUOR_2/3') in combination with a wider range of morphological descriptors to achieve a more refined discrimination between target cells and environmental noise. The integration of fluorescence profiles with detailed morphological parameters was shown to yield superior results in the case of M3.

Comparative analysis demonstrated that M1 achieved high sensitivity for *C. sorokiniana* but was prone to false positives, particularly in contaminated samples, due to its reliance on fluorescence intensity. This overestimation accords with well documented challenges faced in imaging-based cell counting systems such as imaging cytometers (e.g., FlowCam) operating in auto-image mode (Dashkova et al., 2017). In contrast, M2 had greater specificity for *H. pluvialis* by focussing on size and circularity parameters. Nevertheless, it still failed to adequately distinguish aggregates from single cells. M3 outperformed both M1 and M2 by integrating fluorescence and morphological features, dynamically balancing parameter weighting to maintain precise classification across different conditions, effectively reducing overestimation and improving accuracy. In contrast, and in line with findings from fluorescence-enhanced cytometry (Álvarez et al., 2014; Garmendia et al., 2013; Owen et al., 2022), it was found that the combination of multiple fluorescence channels with a higher number of morphological parameters in the M3 model substantially improved counting accuracy.

Operational benchmarking showed that M1 and M2 offered faster processing times (averaging 14.44 ± 1.41 ms per image), while M3 required slightly longer (19.65 ± 1.57 ms per image) due to its more complex multiclass framework. Nonetheless, the additional computational load was justified by its superior accuracy. These findings highlight critical trade-offs between model specialisation and generalisation.

3.3. Validation

The 3 models were validated using a series of cultures that contained different cell concentrations of *C. sorokiniana* and *H. pluvialis* cells. HF3 calculated the total cell concentration in each case as well as the percentage of cells labelled as either *C. sorokiniana* or *H. pluvialis*. The results from the model validations are shown in Fig. 3. Fig. 3A and G shows the accuracy of the three models in quantifying microalgal cell monocultures containing only *C. sorokiniana* or *H. pluvialis,* while Fig. 3B–F shows the accuracy of the different models in quantifying cells in a polyculture containing both species over a range of different cell concentration ratios. When examining cultures containing only *C. sorokiniana* or *H. pluvialis* cells, all three models gave results comparable to those of NCC. However, when the cultures consisted of a mixture of *C. sorokiniana* and *H. pluvialis*, the cell concentrations were model dependent ($p < 0.05$). Overall, the M1 model overestimated the total cell concentration, especially in mixed cultures that had higher concentrations of *H. pluvialis* ($p < 0.05$). For example, the difference between HF3 and NCC was around 100 % in cultures containing 10 % *C. sorokiniana* and 90 % *H. pluvialis* and around 10 % in the culture containing 90 % *C. sorokiniana* and 10 % *H. pluvialis* ($p < 0.05$). Still, this value was higher than expected for a model developed using *C. sorokiniana*. In addition, the M1 model identified small particles with no fluorescence as *C. sorokiniana* which led to an overestimate of the total cell count. In turn, the M2 model accurately quantified the total number of cells similar to NCC. As *H. pluvialis* cells are larger, the model did not identify small particles as cells, unlike M1. No statistical differences were observed between M2 and NCC, where differences were less than 10 % for all the different culture ratios that were tested. No differences were observed in cell counts when using M3 and NCC, regardless of the culture used. Table 1 shows the accuracy of the models in quantifying the abundance of *C. sorokiniana* and *H. pluvialis* in the different cultures. Overall, the models were able to identify the presence of the different species, and which was the dominant species in each culture. The M1 model was more accurate in cultures where *C. sorokiniana* cells were the dominant species. The difference between the *C. sorokiniana* cell concentration measured using HF3 and NCC was approximately 5 % and 7 % in cultures where *C. sorokiniana* cells represented 75 % and 90 % of the cells respectively. In turn, when just 10 % of the cells were *C. sorokiniana*, the HF3 system recognised 58.8 % of the cells as *C. sorokiniana*. As mentioned above, the system recognised some particles with no fluorescence as *C. sorokiniana* along with some *H. pluvialis* as groups of *C. sorokiniana* cells. The same difference was observed when analysing the culture using the M2 model. This model, which was developed using *H. pluvialis* monocultures, recognised that the culture containing 10 % *C. sorokiniana* cells was made up of *H. pluvialis* (56.5 %) and other objects, including *C. sorokiniana*

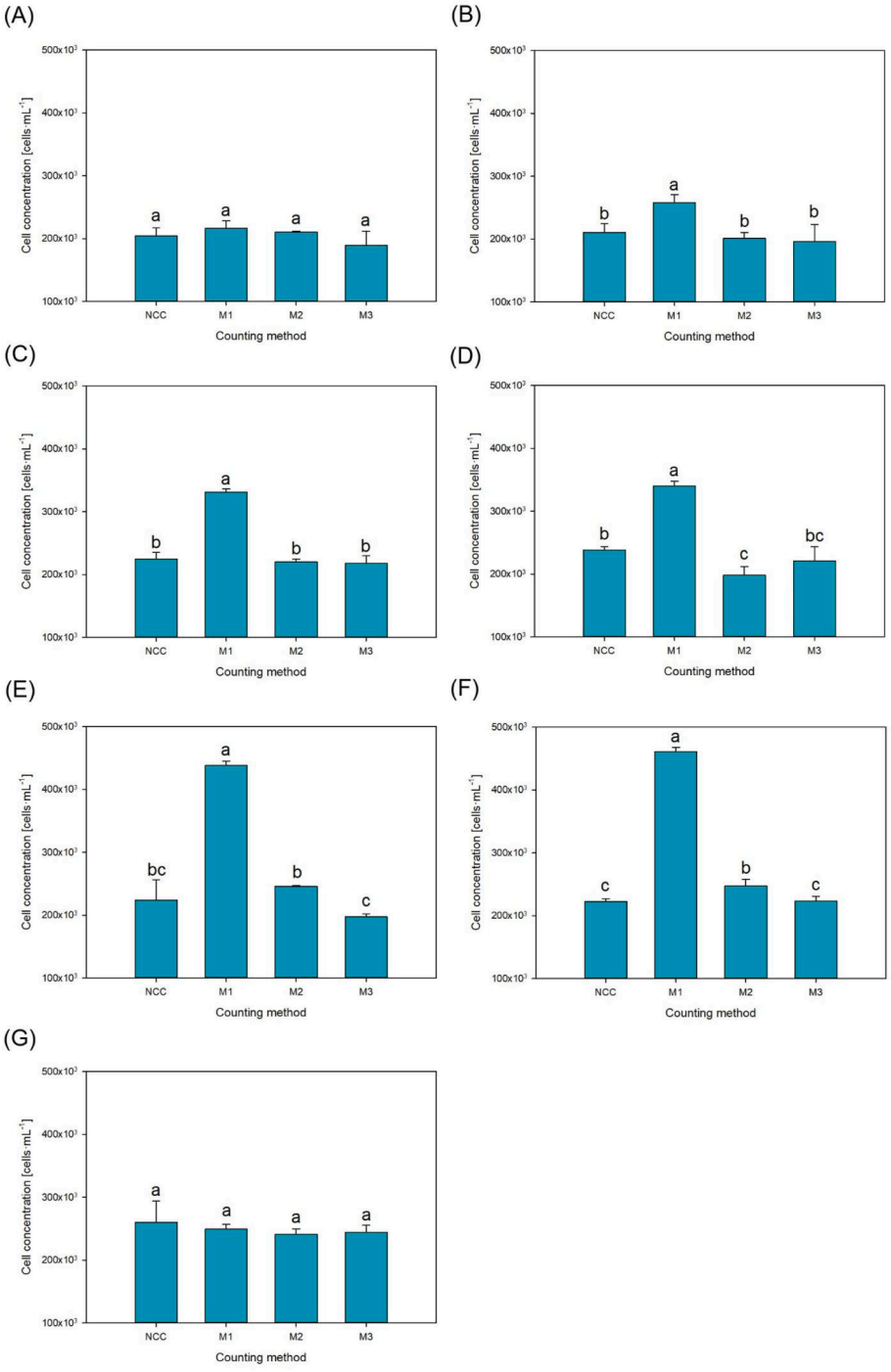

Fig. 3. Cell count in cultures of (**A**) 100 % *C. sorokiniana*, (**B**) 90 % *C. sorokiniana* and 10 % *Haematococcus* cells, (**C**) 75 % *C. sorokiniana* and 25 % *Haematococcus* cells, (**D**) 50 % *C. sorokiniana* and 50 % *Haematococcus* cells, (**E**) 25 % *C. sorokiniana* and 75 % *H. pluvialis* cells, (**F**) 10 % *C. sorokiniana* and 90 % *H. pluvialis* cells, and (**G**) 100 % *H. pluvialis* cells. HF3 and NCC refer to HOLODETECT HiRes + FLUOR3 and Neubauer counting chamber, respectively. The results are the average of five independent determinations ± SD.

(43.5 %). This problem was resolved when analysing the cultures using M3—the model that was developed using mixtures of both *C. sorokiniana* and *H. pluvialis*. In this case, the difference between results obtained using HF3 and NCC was minimal, and the results had a positive correlation for both the *C. sorokiniana* ($p < 0.05$; 0.9791) and *H. pluvialis* ($p < 0.05$; 0.9790) cultures. The M3 model proved to be accurate, especially when monocultures were analysed, identifying 99.9 % of the *C. sorokiniana* cells and 95.9 % of the *H. pluvialis* cells in the monocultures respectively.

The validation results presented above highlight the HF3 system's strengths in identifying and quantifying microalgae in both monocultures and polycultures. This shows that the HF3 system is a valuable alternative to other image-based systems, such as FlowCam. FlowCam relies on two-dimensional imaging, fluorescence triggering and flow cytometry (Otálora et al., 2023), which can limit its effectiveness in dense cultures or when distinguishing between morphologically similar species. In contrast, HF3 combines high-resolution digital holography with fluorescence. Although HF3 needs sample dilution for small cells at high cell concentrations and takes longer to process complex models, its accuracy and flexibility make it a strong contender for monitoring microalgae.

Table 1
Model validation: Abundance of *C. sorokiniana* and *H. pluvialis* cells in monocultures and polycultures. The results are the average of five independent determinations ± SD.

Culture[a]	M1		M2		M3	
	C. sorokiniana (%)	*Others* (%)	*Others* (%)	*H. pluvialis* (%)	*C. sorokiniana* (%)	*H. pluvialis* (%)
100 %C	89.3 ± 1.9	10.6 ± 1.9	99.9 ± 0.0	0.1 ± 0.0	99.9 ± 0.0	0.0 ± 0.0
90 %C–10 %H	82.5 ± 1.3	17.5 ± 1.3	91.1 ± 1.3	8.9 ± 1.3	89.0 ± 3.9	10.9 ± 3.9
75 %C–25 %H	70.7 ± 1.2	29.3 ± 1.2	78.5 ± 1.3	21.5 ± 1.3	66.5 ± 1.7	33.5 ± 1.7
50 %C–50 %H	64.9 ± 1.5	35.1 ± 1.5	66.9 ± 2.1	33.1 ± 2.1	40.9 ± 1.8	59.1 ± 1.8
25 %C–75 %H	58.9 ± 2.5	41.1 ± 2.5	48.3 ± 2.3	51.7 ± 2.3	13.6 ± 1.4	86.4 ± 1.4
10 %C–90 %H	58.83 ± 1.5	41.2 ± 1.5	43.5 ± 3.8	56.5 ± 3.8	8.7 ± 1.3	91.3 ± 1.3
100 %H	25.6 ± 6.4	73.2 ± 5.6	38.9 ± 0.0	61.1 ± 8.4	4.1 ± 2.9	95.9 ± 2.9

[a] C and H refer to *C. sorokiniana* and *H. pluvialis,* respectively. The percentages represent the relative abundance of cells of each species.

4. Conclusions

High-resolution holographic reconstruction combined with fluorescence microscopy was used to calculate the cellular concentration of monocultures and polycultures of *C. sorokiniana* and *H. pluvialis*. This technology permitted accurate cell counts in cultures of *C. sorokiniana* and *H. pluvialis* and allows the quantification of the abundance of each species independently. Three models called M1, M2 and M3 were developed. M3, where the two species were considered independently in mixed cultures, provided the best results, allowing the rapid quantification of the abundance of each species to obtain cell concentration results comparable to those of a Neubauer counting chamber. The main limitation in *C. sorokiniana* cultures was the need for dilution, as high cell concentrations led to inaccurate results. Future work will focus on developing novel models that include other species, thus allowing the full characterisation of cultures containing more than two species.

CRediT authorship contribution statement

María Salinas-García: Writing – original draft, Validation, Investigation, Formal analysis. **Barbara Bicsák:** Investigation. **Gabriel Acién:** Writing – review & editing, Supervision, Funding acquisition, Conceptualization. **Tomás Lafarga:** Supervision, Funding acquisition, Formal analysis.

Funding

This work was funded by the European Union and forms part of the projects NIAGARA (Grant agreement: 101146861), COSEC (Grant agreement: 101172850), and ALLIANCE (Grant agreement: 101214199). This work is also part of SOLAR·FOODS and SHAPE (PID2022-136292OB-I00; CNS2024-154218), funded by the Spanish Ministry of Science and Innovation and the European Union, and BLUE·FUTURE and RE·USE (PCM_00083; PLSQ_2023_00233), funded by the Government of Andalusia and the European Union. Tomás Lafarga would like to thank the Ramon y Cajal Program (RYC2021-031061-I) funded by the Spanish Ministry of Science and Innovation and the European Union.

Data availability

Data will be made available by the corresponding author on request.

Declaration of competing interest

The authors declare the following financial interests/personal relationships which may be considered as potential competing interests: Barbara Bicsák was employed by Holodetect Instruments Ltd. (Budapest, Hungary) during the experiments. The other authors declare that they have no known competing interests or personal relationships that could have appeared to influence the work reported in this paper.

References

Álvarez, E., López-Urrutia, Á., Nogueira, E., Fraga, S., 2011. How to effectively sample the plankton size spectrum? A case study using FlowCAM. J. Plankton Res. 33 (7), 1119–1133. https://doi.org/10.1093/PLANKT/FBR012.

Álvarez, E., Moyano, M., López-Urrutia, Á., Nogueira, E., Scharek, R., 2014. Routine determination of plankton community composition and size structure: a comparison between FlowCAM and light microscopy. J. Plankton Res. 36 (1), 170–184. https://doi.org/10.1093/plankt/fbt069.

Baroni, É.G., Yap, K.Y., Webley, P.A., Scales, P.J., Martin, G.J.O., 2019. The effect of nitrogen depletion on the cell size, shape, density and gravitational settling of *Nannochloropsis salina, Chlorella* sp. (marine) and *Haematococcus pluvialis*. Algal Res. 39, 101454. https://doi.org/10.1016/J.ALGAL.2019.101454.

Chen, Y., Wang, Q., Xue, J., Yang, Y., Wu, H., 2023. Applicability of flow imaging microscopy (FlowCAM) as a ballast water investigation tool. Reg. Stud. Mar. Sci. 60, 102821. https://doi.org/10.1016/J.RSMA.2023.102821.

Colusse, G.A., Mendes, C.R.B., Duarte, M.E.R., Carvalho, J. C. de, Noseda, M.D., 2020. Effects of different culture media on physiological features and laboratory scale production cost of *Dunaliella salina*. Biotechnology Reports 27, e00508. https://doi.org/10.1016/J.BTRE.2020.E00508.

Dashkova, V., Malashenkov, D., Poulton, N., Vorobjev, I., Barteneva, N.S., 2017. Imaging flow cytometry for phytoplankton analysis. Methods 112, 188–200. https://doi.org/10.1016/j.ymeth.2016.05.007.

Di Caprio, F., 2020. Methods to quantify biological contaminants in microalgae cultures. Algal Res. 49, 101943. https://doi.org/10.1016/J.ALGAL.2020.101943.

Ding, Y., Zhang, A., Wen, X., Wang, Z., Wang, K., Geng, Y., Li, Y., 2020. Application of surfactants for controlling destructive fungus contamination in mass cultivation of *Haematococcus pluvialis*. Bioresour. Technol. 317, 124025. https://doi.org/10.1016/J.BIORTECH.2020.124025.

Garmendia, M., Revilla, M., Zarauz, L., 2013. Testing the usefulness of a simple automatic method for particles abundance and size determination to derive cost-effective biological indicators in large monitoring networks. Hydrobiologia 704 (1), 231–252. https://doi.org/10.1007/s10750-012-1400-x.

González-Hernández, J., Ciardi, M., Guzmán, J.L., Moreno, J.C., Acién, F.G., 2025. A low-cost methodology based on artificial intelligence for contamination detection in microalgae production systems. Algal Res. 85, 103849. https://doi.org/10.1016/J.ALGAL.2024.103849.

Havlik, I., Reardon, K.F., Ünal, M., Lindner, P., Prediger, A., Babitzky, A., Beutel, S., Scheper, T., 2013. Monitoring of microalgal cultivations with on-line, flow-through microscopy. Algal Res. 2 (3), 253–257. https://doi.org/10.1016/J.ALGAL.2013.04.001.

Huang, Y., Liu, J., Wang, H., Gao, Z., 2014. Treatment potential of a synergistic botanical pesticide combination for rotifer extermination during outdoor mass cultivation of *Spirulina platensis*. Algal Res. 6 (PB), 139–144. https://doi.org/10.1016/J.ALGAL.2014.11.003.

Hwang, S.W., Choi, H. Il, Sim, S.J., 2019. Acidic cultivation of *Haematococcus pluvialis* for improved astaxanthin production in the presence of a lethal fungus. Bioresour. Technol. 278, 138–144. https://doi.org/10.1016/J.BIORTECH.2019.01.080.

Jaffari, Z.H., Na, S., Abbas, A., Park, K.Y., Cho, K.H., 2024. Digital imaging-in-flow (FlowCAM) and probabilistic machine learning to assess the sonolytic disinfection of Cyanobacteria in sewage wastewater. J. Hazard Mater. 468, 133762. https://doi.org/10.1016/J.JHAZMAT.2024.133762.

Morillas-España, A., Lafarga, T., Gómez-Serrano, C., Acién-Fernández, F.G., González-López, C.V., 2020. Year-long production of *Scenedesmus almeriensis* in pilot-scale raceway and thin-layer cascade photobioreactors. Algal Res. 51, 102069. https://doi.org/10.1016/j.algal.2020.102069.

Otálora, P., Guzmán, J.L., Acién, F.G., Berenguel, M., Reul, A., 2023. An artificial intelligence approach for identification of microalgae cultures. New Biotechnology 77, 58–67. https://doi.org/10.1016/J.NBT.2023.07.003.

Owen, B.M., Hallett, C.S., Cosgrove, J.J., Tweedley, J.R., Moheimani, N.R., 2022. Reporting of methods for automated devices: a systematic review and recommendation for studies using FlowCam for phytoplankton. Limnol Oceanogr. Methods 20 (7), 400–427. https://doi.org/10.1002/lom3.10496.

Paszke, A., Gross, S., Massa, F., Lerer, A., Bradbury, J., Chanan, G., Killeen, T., Lin, Z., Gimelshein, N., Antiga, L., Desmaison, A., Köpf, A., Yang, E., DeVito, Z., Raison, M., Tejani, A., Chilamkurthy, S., Steiner, B., Fang, L., Bai, J., Chintala, S., 2019. PyTorch:

an imperative style, high-performance deep learning library. Adv. Neural Inf. Process. Syst. 32. http://arxiv.org/abs/1912.01703.

Sarrafzadeh, M.H., La, H.J., Seo, S.H., Asgharnejad, H., Oh, H.M., 2015. Evaluation of various techniques for microalgal biomass quantification. J. Biotechnol. 216, 90–97. https://doi.org/10.1016/J.JBIOTEC.2015.10.010.

Takahashi, T., 2019. Routine management of microalgae using autofluorescence from chlorophyll. Molecules 24. https://doi.org/10.3390/MOLECULES24244441.

UNE, 2022. Algae and Algae Products – Methods of Sampling and Análisis – Sample Treatment (UNE-EN 17605:2002).

Villaró, S., Acién, G., González-López, C.V., Clagnan, E., Lafarga, T., 2023. Production of *Arthrospira platensis* BEA 005B: biomass characterisation and use as a colouring additive in macarons. LWT 182, 114843. https://doi.org/10.1016/J.LWT.2023.114843.

Villaró, S., Sánchez-Zurano, A., Ciardi, M., Alarcón, F.J., Clagnan, E., Adani, F., Morillas-España, A., Álvarez, C., Lafarga, T., 2022. Production of microalgae using pilot-scale thin-layer cascade photobioreactors: effect of water type on biomass composition. Biomass Bioenergy 163, 106534. https://doi.org/10.1016/J.BIOMBIOE.2022.106534.

Villaró-Cos, S., Guzmán Sánchez, J.L., Acién, G., Lafarga, T., 2024. Research trends and current requirements and challenges in the industrial production of spirulina as a food source. Trends Food Sci. Technol. 143, 104280. https://doi.org/10.1016/J.TIFS.2023.104280.

Wang, J., Liu, K., Zhang, Y., Leng, B., Lu, J., 2023. Recent advances of few-shot learning methods and applications. Sci. China Technol. Sci. 66 (4), 920–944. https://doi.org/10.1007/s11431-022-2133-1.

Yourassowsky, C., Theunissen, R., Dohet-Eraly, J., Dubois, F., 2024. Lipid quantification in living microalgal cultures with digital holographic microscopy. Frontiers in Photonics 4, 1301708. https://doi.org/10.3389/FPHOT.2023.1301708/BIBTEX.

Yu, B.S., Lee, S.Y., Sim, S.J., 2022. Effective contamination control strategies facilitating axenic cultivation of *Haematococcus pluvialis*: risks and challenges. Bioresour. Technol. 344, 126289. https://doi.org/10.1016/J.BIORTECH.2021.126289.

Zhang, C., Liu, J., Zhang, L., 2017. Cell cycles and proliferation patterns in *Haematococcus pluvialis*. Chin. J. Oceanol. Limnol. 35 (5), 1205–1211. https://doi.org/10.1007/s00343-017-6103-8.